ISSN 0967-0912, Steel in Translation, 2021, Vol. 51, No. 2, pp. 88–92. © Allerton Press, Inc., 2021.
Russian Text © The Author(s), 2021, published in Izvestiya Vysshikh Uchebnykh Zavedenii, Chernaya Metallurgiya, 2021, No. 2, pp. 143–148.

Calculation of Temperature and Thermoelastic Stresses in the Backups with Collars of the Unit of Combined Continuous Casting and Deformation in Steel Billet Production. Report 2

O. S. Lekhov[a], * and A. V. Mikhalev[b]

[a] *Russian State Professional Pedagogical University, Ekaterinburg, 620012 Russia*

[b] *OAO Ural Pipe Plant, Pervoural'sk, Sverdlovsk oblast, 623107 Russia*

**e-mail: MXLehov38@yandex.ru*

Received December 16, 2019

Abstract—The problem statement and boundary conditions for calculation of axial thermoelastic stresses in backups with unit collars of combined continuous casting and deformation are provided for production of three steel billets. The calculation scheme for determination of thermoelastic stresses in backups with collars in a known temperature field was stated using ANSYS software. The calculation results of thermoelastic stresses in shaped dies were performed in four sections of a backup with collars. In each section, calculation results are given for four typical lines and seven points. Values of axial thermoelastic stresses for seven typical points of each section are given for the contact surface of a backup with collars and the contact layer at a depth of 5 mm from the contact surface. The stress state of a shaped backup in the middle of depression between the middle collars was determined and the distribution regularities of axial and equivalent stresses over the thickness, length and width of a backup were established during slab compression and at idle. The calculation results of thermoelastic stresses in the top of the middle collar of a shaped backup on the contact surface and in the contact layer during slab compression and at idle are presented. Graphs of thermoelastic stress distribution along the line passing through the top of a collar are given, which show the zones of compressive and tensile thermoelastic stresses during slab compression and at idle. The character of the stress state in the base of extreme collar was determined for production of three steel billets in the unit of combined process of continuous casting and deformation.

Keywords: unit, continuous casting, deformation, shaped die, collar, billet, temperature, finite element, thermoelastic stress

DOI: 10.3103/S0967091221020042

INTRODUCTION

The work [1] presents the results of calculating the temperature of the backups with unit collars of combined continuous casting and deformation when obtaining three steel billets. For the calculated temperature fields, it is necessary to determine the axial thermoelastic (*SX*, *SY*, *SZ*) and equivalent (*SEQV*) stresses arising in the shaped backups during slab compression and cooling them with water at idle.

STATEMENT OF THE PROBLEM AND BOUNDARY CONDITIONS

The material of the backup is steel of the grade 4X4VMFS. By virtue of symmetry, for the calculation of thermoelastic stresses, half of the backup is taken [1]. In addition to the temperature load on the backup, the kinematic boundary conditions are also applied:

— on the *XY* surface, there is no displacement in the direction of the *Z* axis, which is due to the symmetry of the computational model [1];

— on the rear surface of the backup in contact with the support, the absence of displacements in all directions is set.

CALCULATION METHOD

Since the temperature field of the backup is known, the resolving equations [2–9] make it possible to find the temperature displacements in all nodes of the finite element partition, and then determine the temperature deformations and thermoelastic stresses. The presented scheme for performing calculations by the finite element method is implemented in the ANSYS package [10–20].

The results of calculating thermoelastic stresses in backups are given in four sections [1]. In this case, in

each section, the calculation results are given for four characteristic lines and points (Fig. 1).

CALCULATION RESULTS

The results of calculating the axial and equivalent thermoelastic stresses from the impact on the backup of the heat flow and water cooling at the characteristic points of the P4 lines are given in Table 1.

Specific stress values for seven points of section *4* (points *0*–*6*) on the contact surface of the backup are presented in Table 1. Table 2 shows the stress values in the middle of the depression between the middle collars (points *0* and *0_5*), at the top of the middle collar (points *2* and *2_5*).

The presented results characterize the distribution of axial and equivalent thermoelastic stresses both over the thickness and over the height and width of the backup during slab compression and at idle.

Let us first consider the stress state in the middle of the depression between the middle collars along the thickness and height of the backup (Table 2). The middle of the depression between the middle collars is in the *XY* plane at $Z = 0$ (Fig. 1, the plane of symmetry).

The presented results indicate that in the middle of the depression between the collars in the contact zone of the backup with the workpiece, from the effect of the temperature load in the near-contact layer of the backup, compressive stresses arise, which have maximum values on the contact surface (Table 2). The maximum thermoelastic stresses arise along the *Z* axis and reach –968 MPa in section *4* along the T4V line (Table 2). Then, the compressive stresses along the backup thickness decrease and reach their minimum values at a depth of 5 mm of the near-contact layer (Table 2).

The maximum stresses in the direction of the *Z* axis at a depth of 5 mm do not exceed –258 MPa. Equivalent stresses on the contact surface of the backup change in the middle of the depression between the collars in the range of 607–813 MPa, and at a depth of 5 mm—in the range of 84–238 MPa.

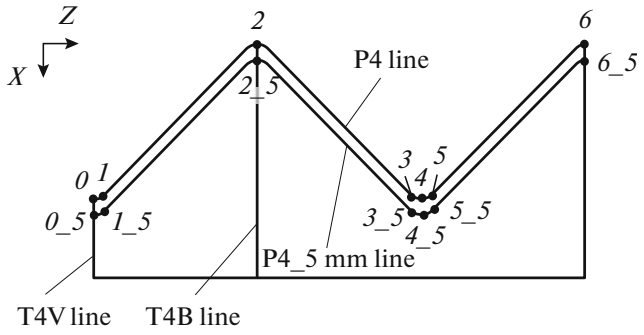

Fig. 1. Position of lines in section *4*.

Consider the stress state at the top of the middle collar (Table 2, Fig. 1). The presented results indicate that at the top of the middle collar in the contact zone of the backup with the slab from the effect of the temperature load on the contact surface and in the near-contact layer of the backup, compressive stresses arise (Table 2, Fig. 1). The maximum thermoelastic stresses arise along the *Y* axis and reach a value of –530 MPa in section 1 along the T1B line (Table 2). Then, the compressive stresses in thickness decrease (as for the zone of the depression between the collars). In this case, stresses along the *X* axis at a depth of 5 mm from the contact layer from compressive stresses to tensile ones (for the T1B, T2B and T3B lines). For the T4B line, the stresses along the *X* axis are tensile both at the contact surface and at a depth of 5 mm. However, the level of these tensile stresses is low and does not exceed 62 MPa. Stresses along the *Y* axis, as well as stresses along the *X* axis, change from compressive stresses to

Table 1. Axial and equivalent stresses at the points of the P4 line from the impact of the heat flow (HF) and water cooling (WC) on a backup

Point	Stress, MPa, at the end of the pause (WC)/at the end of the contact (HF)			
	SX	*SY*	*SZ*	*SEQV*
0	–18/–37	–128/–593	–488/–968	427/813
1	–69/–150	–115/–576	–413/–849	408/808
2	–3/13	128/–243	69/–242	118/262
3	–46/–128	–75/–536	–267/–706	282/688
4	–10/–29	–73/–538	–266/–744	247/643
5	–29/–108	–56/–513	–183/–610	195/604
6	1/–7	91/–257	0/–4	93/257
Maximum	–23/–46	–130/–594	–493/–976	432/820

In the figures and tables, the stresses arising at the end of the pause (at idle) are designated "WC", and at the end of the contact (compression)—"HF".

Table 2. Axial and equivalent stresses at the points of the T1V–T4V and T1B–T4B lines from the impact of heat flow (HF) and water cooling (WC) on a backup

Point	Stress, MPa, at the end of the pause (WC) / at the end of the contact (HF)			
	SX	*SY*	*SZ*	*SEQV*
	on the T1V line			
0	0/0	−106/−582	−154/−629	137/607
0_5	1/1	−205/−186	−247/−230	230/213
	On the T2V line			
0	0/0	−144/−619	−173/−640	160/630
0_5	−3/−2	−241/−225	−272/−252	255/238
	On the T3V line			
0	0/0	−95/−565	−224/−665	195/621
0_5	−39/−43	−189/−172	−279/−258	210/188
	On the T4V line			
0	−18/−37	−128/−593	−488/−968	427/813
0_5	−106/−147	−148/−139	−233/−210	121/84
	On the T1B line			
2	−12/−31	−102/−530	85/−260	168/507
2_5	−44/46	−245/−184	−79/−53	214/235
	On the T2B line			
2	−9/−28	−75/−503	85/−261	143/482
2_5	−50/39	−228/−168	−23/1	209/215
	On the T3B line			
2	5/−14	103/−322	83/−260	104/326
2_5	−35/54	−83/−12	−17/4	59/60
	On the T4B line			
2	−3/13	128/−243	69/−242	118/262
2_5	−46/62	−30/53	−20/13	26/47

tensile ones, but only for the T4B line. The presented results indicate that the bottom of the backup at the top of the middle collar at a depth of 5 mm from the effect of temperature during the working operation is in conditions of comprehensive stress, however, the level of these stresses in the direction of the *X* axis does not exceed 62 MPa (Table 2, line T4B). The contact surface of the middle collar is in conditions of all-round compression, with the exception of the transition zone of the backup into the shaping section. Equivalent stresses on the contact surface of the backup change at the top of the collar in the range of 262–507 MPa, and at a depth of 5 mm—in the range of 47–235 MPa.

Let us consider the distribution of axial stresses in the near-contact layer at the top of the middle collar when the backup is cooled with water at idle (Table 2, Fig. 2).

The stress state of the near-contact layer at the top of the middle collar is characterized by the presence of both compressive and tensile stresses. The maximum stresses are along the *Y* and *Z* axes. In this case, the level of compressive stresses on the contact surface is in the range of −7–102 MPa, and of tensile stresses −69–128 MPa. A specific feature of the stress state is that the contact surface from section 3 to the shaping section is under conditions of comprehensive stress. From section 3 to the zone of the beginning of the deformation zone, it has tensile stresses along the *Z* axis. At a depth of 5 mm, all axial stresses are compressive and do not exceed 245 MPa.

Figure 3 shows a graph of the thermoelastic stress distribution along the *NB–KB* line, which passes along the top of the separating collar during slab compression.

Thermoelastic stresses during slab compression in the direction of the *Y* and *Z* axes are compressive and reach the highest values of −530 and −261 MPa (Fig. 3).

Figure 4 shows the distribution regularities of axial thermoelastic stresses along the *RN–RK* line, which is located at the base of the extreme collar during slab

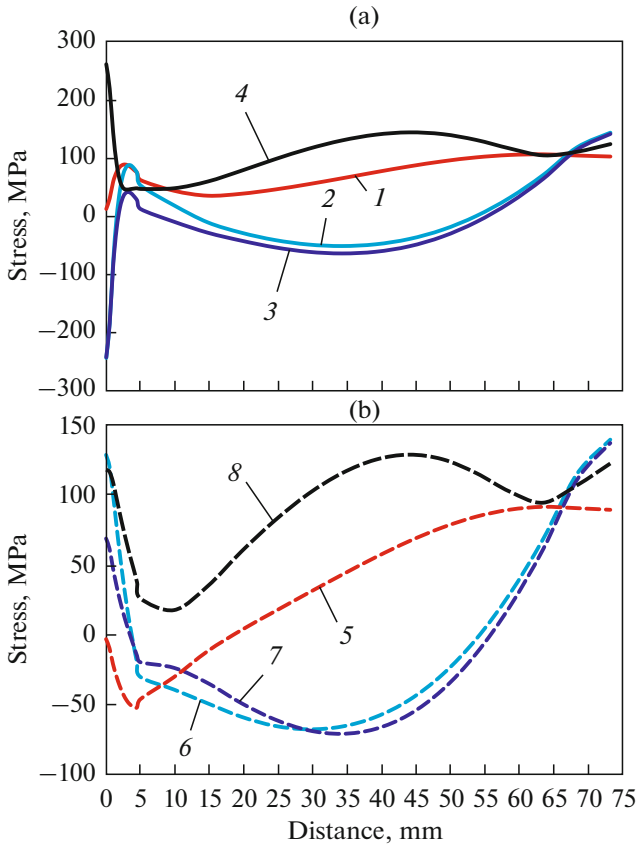

Fig. 2. Nature of temperature stresses along the T4B line from the heat flow (HF) (a) and water cooling (WC) (b) impact on a backup: (*1*) *SX*_HF_T4B; (*2*) *SY*_HF_T4B; (*3*) *SZ*_HF_T4B; (*4*) *SEQV*_HF_T4B; (*5*) *SX*_WC_T4B; (*6*) *SY*_WC_T4B; (*7*) *SZ*_WC_T4B; (*8*) *SEQV*_WC_T4B.

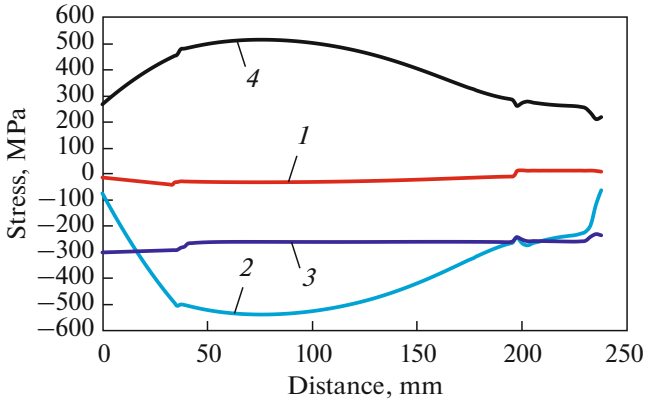

Fig. 3. Nature of thermoelastic stresses along the *NB–KB* line from the impact of heat flow (HF) on a backup: (*1*) *SX*_HF_*NB–KB*; (*2*) *SY*_HF_*NB–KB*; (*3*) *SZ*_HF_*NB–KB*; (*4*) *SEQV*_HF_*NB–KB*.

compression and at idle. When the slab is compressed, all axial thermoelastic stresses are compressive and in the direction of the *Z* axis reach the maximum value of 610 MPa in section *4*.

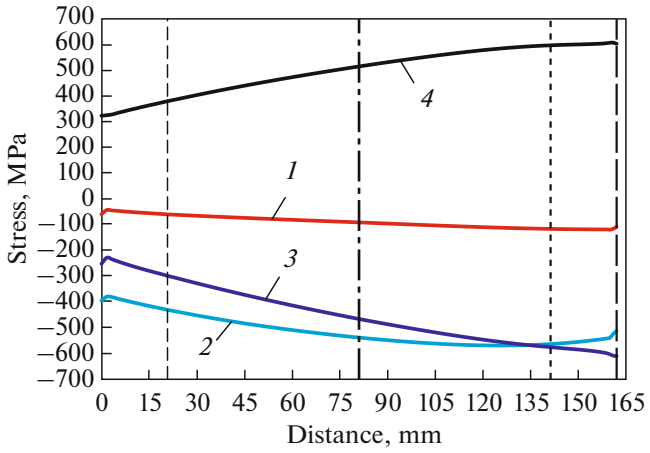

Fig. 4. Nature of thermoelastic stresses along the *RN–RK* line from the impact of heat flow (HF) on a backup: (*1*) *SX*_HF_*RN–RK*; (*2*) *SY*_HF_*RN–RK*; (*3*) *SZ*_HF_*RN–RK*; (*4*) *SEQV*_HF_*RN–RK*. (–––) Section *1*; (– – –) section *2*; (---) section *3*; (——) section *4*.

CONCLUSIONS

The problem of determining the thermoelastic stresses in the backups with unit collars of combined continuous casting and deformation during the production of three steel billets has been posed and solved in a three-dimensional formulation. The distribution regularities of axial and equivalent thermoelastic stresses on the contact surface and in the near-contact layer of the shaped backup of the unit of combined continuous casting and deformation have been established.

REFERENCES

1. Lekhov, O.S. and Mikhalev, A.V., Calculation of temperature and thermoelastic stresses in the backups with unit collars of combined continuous casting and deformation during steel billet production. Report 1, *Steel Transl.*, 2020, vol. 50, no. 12, pp. 877–881. https://doi.org/10.3103/S0967091220120086
2. Lekhov, O.S., Mikhalev, A.V., and Shevelev, M.M., *Napryazheniya v sisteme boiki-polosa pri poluchenii listov iz stali na ustanovke nepreryvnogo lit'ya i deformatsii* (Stresses in the Backup-Strip System when Making Steel Sheets at Unit of Continuous Casting and Deformation), Yekaterinburg: Ural. Metod. Tsentr, Ural. Politekh. Inst., 2018.
3. Khloponin, V.N., Kosyreva, M.V., and Kosyak, A.S., Influence of cooling system on thermal conditions of roller surface work, *Tr. Mosk. Inst. Stali Splavov*, 1977, no. 100, pp. 90–93.
4. Boley, B.A. and Weiner, J.H., *Theory of Thermal Stresses*, New York: Wiley, 1960.
5. Lekhov, O.S., Study of stress-strain state of rolls-band system at rolling of broad-flanged beam in stands of universal beam mill: Report 2, *Izv. Vyssh. Uchebn. Zaved., Chern. Metall.*, 2014, vol. 57, no. 12, pp. 15–19.

6. Kushner, V.S., Vereshchaka, A.S., Skhirtladze, A.G., and Negrov, D.A., *Tekhnologicheskie protsessy v mashinostroenii. Chast' 2. Obrabotka metallov davleniem i svarochnoe proizvodstvo* (Technological Processes in Mechanical Engineering, Part 2: Metal Forming and Welding), Omsk: Omsk. Gos. Tekh. Univ., 2005.
7. Bulanov, L.V., Karlinskii, S.E., and Volegova, V.E., Durability of CCM rolls at external and internal cooling, in *Nadezhnost' krupnykh mashin* (Reliability of Large Machines), Sverdlovsk: Nauchno-Issled. Inst. Tyazh. Mashinostr., 1990, pp. 126–132.
8. Lykov, A.V., *Teoriya teploprovodnosti* (Theory of Heat Conduction), Moscow: Vysshaya Shkola, 1967.
9. Singh, V. and Das, S.K., Thermo-fluid mathematical modeling of steel slab casters: progress in 21st century, *ISIJ Int*., 2016, vol. 56, no. 9, pp. 1509–1518. https://doi.org/10.2355/isijinternational.ISIJINT-2015-620
10. *ANSYS Mechanical APDL Structural Analysis Guide, Release 15.0*, Canonsburg, PA: ANSYS, 2013.
11. Matsumia, T. and Nakamura, Y., Mathematical model of slab bulging during continuous casting, *Proc. 3rd Process Technology Conf. "Applied Mathematical, and Physical Models in Iron and Steel Industry," Pittsburgh, Pa, March 28–31, 1982*, New York, 1982, pp. 264–270.
12. Takashima, Y. and Yanagimoto, I., Finite element analysis of flange spread behavior in H-beam universal rolling, *Steel Res. Int*., 2011, vol. 82, no. 10, pp. 1240–1247. https://doi.org/10.1002/srin.201100078
13. Kobayashi, S., Oh, S.-I., and Altan, T., *Metal Forming and Finite Element Method*, Oxford: Oxford Univ. Press, 1989.
14. Karrech, A. and Seibi, A., Analytical model of the expansion in tubes under tension, *J. Mater. Process. Technol.*, 2010, vol. 210, no. 2, pp. 336–362. https://doi.org/10.1016/j.jmatprotec.2009.09.024
15. Kazakov, A.L. and Spevak, L.F., Numeral and analytical studies of nonlinear parabolic equation with boundary conditions of a special form, *Appl. Math. Model.*, 2013, vol. 37, nos. 10–13, pp. 6918–6928. https://doi.org/10.1016/j.apm.2013.02.026
16. Jansson, N., Optimized sparse matrix assembly in finite element solvers with one-sided communication, in *High Performance Computing for Computational Science–VECPAR 2012*, Berlin: Springer-Verlag, 2013, pp. 128–139.
17. Park, C.Y. and Yang, D.Y., A study of void crushing in large forgings II. Estimation of bonding efficiency by finite-element analysis, *J. Mater. Process. Technol.*, 1997, vol. 72, no. 1, pp. 32–41. https://doi.org/10.1016/S0924-0136(97)00126-X
18. Sorimachi, K. and Emi, T., Elastoplastic stress analysis of bulging as a major cause of internal cracks in continuously cast slabs, *Tetsu-to-Hagane*, 1977, vol. 63, no. 8, pp. 1297–1304. https://doi.org/10.2355/tetsutohagane1955.63.8_1297

Translated by S. Avodkova